

## **Ranz and Marshall Correlations Limits on Heat Flow Between a Sphere and its Surrounding Gas at High Temperature**

Abderrahmane Aissa, Mohamed Abdelouahab, Abdelkader Noureddine,  
Mohammed El Ganaoui, Bernard Pateyron

► **To cite this version:**

Abderrahmane Aissa, Mohamed Abdelouahab, Abdelkader Noureddine, Mohammed El Ganaoui, Bernard Pateyron. Ranz and Marshall Correlations Limits on Heat Flow Between a Sphere and its Surrounding Gas at High Temperature. *Thermal Science*, VINČA Institute of Nuclear Sciences, 2015, 19 (5), pp.1521-1528. <10.2298/TSCI120912090A>. <hal-01599788>

**HAL Id: hal-01599788**

**<https://hal.univ-lorraine.fr/hal-01599788>**

Submitted on 2 Oct 2017

**HAL** is a multi-disciplinary open access archive for the deposit and dissemination of scientific research documents, whether they are published or not. The documents may come from teaching and research institutions in France or abroad, or from public or private research centers.

L'archive ouverte pluridisciplinaire **HAL**, est destinée au dépôt et à la diffusion de documents scientifiques de niveau recherche, publiés ou non, émanant des établissements d'enseignement et de recherche français ou étrangers, des laboratoires publics ou privés.

## RANZ AND MARSHALL CORRELATIONS LIMITS ON HEAT FLOW BETWEEN A SPHERE AND ITS SURROUNDING GAS AT HIGH TEMPERATURE

by

**Abderrahmane AISSA<sup>a\*</sup>, Mohamed ABDELOUAHAB<sup>a</sup>,  
Abdelkader NOUREDDINE<sup>b</sup>, Mohammed EL GANAOUI<sup>c</sup>,  
and Bernard PATEYRON<sup>d</sup>**

<sup>a</sup>Oran University of Science and Technology – Mohamed Boudiaf, Oran, Algeria

<sup>b</sup>Laboratory for Modelling and Optimization of Industrial Systems, Oran University  
of Science and Technology Mohamed Boudiaf, Oran, Algeria

<sup>c</sup>LERMAB, Institute Carnot, University Henri Poincare, Nancy, France,

<sup>d</sup>CNRS-SPCTS/CEC, Limoges, France

Original scientific paper

DOI:10.2298/TSCI120912090A

*Direct numerical simulations for axisymmetric plasma jet are developed to investigate particle plasma spraying process. In this paper we study the plasma jet and we focus mainly on the plasma-particle exchanges. Finite element analysis employing COMSOL multiphysics software is used in this simulation. Finally, comparisons are made with the numerically observed particle Nusselt's numbers and theoretically predicted Nusselt's numbers based on the Ranz and Marshall correlation. The results agree well with those obtained previously.*

Key words: heat transfer, high temperature, plasma, thermal spraying

### Introduction

Heat transfer from a spherical particle to the surrounding plasma gas occurs in various industrial processes, such as in thermal spray technology, fluidized bed reactors, and slurry reactors. Over the years, a considerable amount of literature has addressed the problem of the fluid-solid interaction in an unconfined region, especially in thermal spray process.

Thermal spraying uses a plasma gas which transports and accelerates fine particles about 5 to 100 micrometers of molten material with a high temperature on a surface coat.

Those droplets are deposited and then are solidified on the substrate. The particle accumulation on the substrate creates a coating. The connections between the substrate and deposited layer are entirely mechanical. The material to be deposited may be in the form of powder, wire or rod. The energy source may be provided with flame or electric arc plasma jet [1-5].

The aim of this work is to determine the heat exchange between the plasma gas and the spherical particle. Indeed, in plasma sprays, metal or ceramic materials (20-60  $\mu$ ) in a molten or semi molten state are projected at high velocity on beforehand prepared substrates. The gas reaches high temperatures ranging from 6000 K to 12000 K and ensuring particle fusion for most refractory materials. The impact velocity of the drops is relatively higher, in the or-

\* Corresponding author; e-mail: aissa86@gmail.com

der of 100 m/s to 500 m/s. It is difficult to describe the behavior during the impact on the substrate [6] which is directly related to the thermal and dynamic particle histories in the flame. This dynamic and thermal behaviors are described by numerical simulations to independently evaluate the axisymmetric jet flow and the particle behavior injected into it [7-11]. The calculations are based on semi empirical transfer laws. This numerical study allows a better understanding of the transfer phenomena as well as the validity range of the semi-empirical correlations.

### Some basic considerations

The dimensionless analysis of the problem suggests that the thermal boundary layer of the particle immersed in high plasma temperature is a reflection of the dynamic boundary layer. The Ranz and Marshall correlation, established in 1952, can explain the heat transfer between a spherical particle and the plasma gas. This correlation can be written:

$$\text{Nu} = h \frac{d_p}{\kappa} = a + c \text{Re}^m \text{Pr}^n \quad (1)$$

where Nu is the Nusselt number for the transfer plasma/particle, Re – the Reynolds number of the particle given by eq. (2), Pr – the Prandtl number of surrounding gases given by eq. (3),  $h$  – the heat coefficient, and  $\kappa$  – the thermal conductivity of the gas. The constants flow properties  $a$ ,  $c$ ,  $n$ , and  $m$  are numerical constant determined by the fluid chosen and the flow geometry.

The Nusselt number  $\text{Nu} = hd_p/\kappa$  characterizes the thermal boundary layer of the particle with diameter  $d_p$ . The latter receiving on its entire surface ( $S = 4\pi d_p^2$ ), at temperature  $T_p$ . The heat flux  $\Phi = hS(T_\infty - T_p)$  of plasma temperature  $T_\infty$ . The heat transfer coefficient  $h$  at the plasma/particle interface is calculated with established empirical correlations of eq. (1): with

$$\text{Re} = \frac{\rho_\infty (V_\infty - V_p) d_p}{\mu} \quad (2)$$

and

$$\text{Pr} = \frac{\mu c_p}{\kappa} \quad (3)$$

In the Ranz and Marshall correlation [8], it is postulated that at fluid velocity ( $V_{\text{in}}$ ) equal zero, heat transfer is effected only by conduction, which leads to a value of  $a = 2$ , by estimating the coefficients  $c$ ,  $m$ , and  $n$  equal to 0.6, 0.5, and 0.33, respectively.

The correct terms are introduced to take into account the effects of temperature gradients in the boundary layer and non-continuity relating to the plasma flows where the mean free path of the molecules is close to the particle diameter. Table 1 summarizes some Nusselt number correlations [8-12].

In order to take account the velocity and forced convection, the Reynolds number is introduced as an additive term. Besides, the Prandtl number is also used to characterize the plasma gas nature and its heat storage capacity. Due to the thermal boundary layer thickness and the high thermal gradient with in it and which generates inhomogeneity terms of properties involving the kinematic or dynamic viscosity ratio product by the density or even specific

heat ratio. Note that Kalganova correlation in [12] weights the Nusselt number of conductive transfer by the thermal conductivity ratio.

In this study, the momentum and energy equations, together with the above appropriate boundary conditions (fig. 1), was solved in a segregated manner using COMSOL Multiphysics software (version 3.5a). The values of the global characteristic quantities such as the Nusselt numbers on the particle surface were obtained through COMSOL post processing. From the obtained values the Nusselt number was computed and compared with the correlations proposed by Ranz and Marshall, Lewis and Gauvin, Fiszdon, Lee and Pfender, and Kalganova (tab. 1).

**Table 1. Empirical correlations used for calculating the Nusselt number [7]**

Ranz and Marshall [8]	$Nu = 2 + 0.6 Re^{0.5} Pr^{0.33}$
Lewis and Gauvin [12]	$Nu = (2 + 0.515 Re^{0.5}) \left( \frac{\rho_{\infty} \mu_{\infty}}{\rho_w \mu_w} \right)^{-0.15}$
Fiszdon [in 9 and 11]	$Nu = (2 + 0.6 Re^{0.5} Pr^{0.33}) \left( \frac{\rho_{\infty} \mu_{\infty}}{\rho_w \mu_w} \right)^{0.6}$
Lee and Pfender [in 11]	$Nu = (2 + 0.6 Re^{0.5} Pr^{0.33}) \left( \frac{\rho_{\infty} \mu_{\infty}}{\rho_w \mu_w} \right)^{0.6} \left( \frac{c_{p\infty}}{c_{pw}} \right)^{0.38}$
Kalganova [in 12]	$Nu = 2 \frac{\kappa_w}{\kappa_{\infty}} + 0.5 Re^{0.5} Pr^{0.4} \left( \frac{\rho_{\infty} \mu_{\infty}}{\rho_w \mu_w} \right)^{0.2}$

**Numerical model**

For a particle in a plasma jet, two characteristics are studied: motion (trajectory, velocity, acceleration) and thermal evolution (temperature, physical state, heat flux). When a particle and a fluid (plasma) are in relative motion, a drag force is given by the fluid to the particle. This force comes from current lines dissymmetry between particle upstream and downstream. This force is given by:

$$F_D = -\frac{1}{2} C_D \pi \frac{d_p^2}{4} \rho_{\infty} |V_{\infty} - V_p| (V_{\infty} - V_p) \quad (4)$$

where  $C_D$  [-] is the drag coefficient that depends of the particle morphology and of Reynolds number,  $d_p$  [m] – the diameter of particle,  $V_{\infty} - V_p$  [ $ms^{-1}$ ] the difference between plasma velocity and particle velocity, and  $\rho_{\infty}$  [ $kgm^{-3}$ ] the plasma density.

Several researchers have shown that in the absence of chemical reactions on the surface, heat conduction convection in the thermal boundary layer is the main mechanism for heating the particle in the plasma jet [1]. While the particle, under plasma condition, is cooled by radiation to the ambient environment.

The convective and conductive heat transfer is described by eq. (5):

$$\rho c_p \frac{dT}{dt} + \rho c_p V \nabla T = \nabla(\kappa \nabla T) + q \quad (5)$$

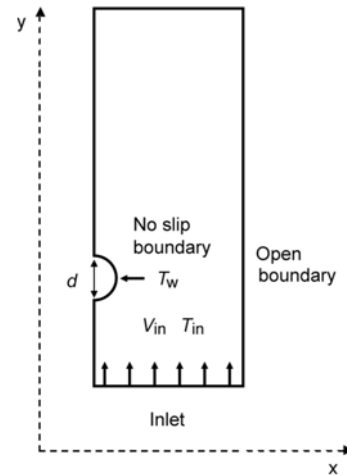


**Figure 1. Initial and boundary conditions used in our model**

where  $c_p$  [ $\text{Jkg}^{-1}\text{K}^{-1}$ ] is the heat capacity,  $\kappa$  [ $\text{Wm}^{-1}\text{K}^{-1}$ ] – the thermal conductivity, and  $V$  – the field velocity calculated by the incompressible Navier-Stokes model. For transport by conduction and convection, the thermal flux vector is given by:

$$q = -\kappa\nabla T + \nabla c_p T V \quad (6)$$

Also the heat flux  $q_r$  due to thermal radiation from the particle to the plasma was  $q_r = \varepsilon\sigma(T_s^4 - T_\infty^4)$ , where  $\varepsilon$  is the emissivity for thermal radiation and  $\sigma$  – the Stefan Boltzmann constant for thermal radiation.

The dimensionless boundary conditions are given as follows (see fig. 1).

*The boundary inlet.* The fluid comes into uniform flow condition and the radial pressure gradient is zero:

$$V_x = 0, \quad V_y = V_\infty, \quad V_z = 0, \quad \frac{dp}{dx} = 0$$

*At the sphere surface.* No-slip condition of the fluid and surface temperature maintained constant at  $T_w$ :

$$V_x = V_y = V_z = 0, \quad r = r_s, \quad T = T_w$$

*In the plasma jet.* Far from the particle the temperature is uniform and equals  $T_\infty$ :

$$r \rightarrow \infty, \quad T = T_\infty$$

The pressure at the outlet is defined as constant, ( $p = p_\infty = p_{\text{atm}}$ ).

The initial condition for the temperature at the particle surface is the same in the whole simulation and it is equal to  $T_w = 300$  K.

The Reynolds and the Prandtl numbers vary with the velocities ( $V_{\text{in}}$ ) and temperatures ( $T_{\text{in}}$ ) of the gas.

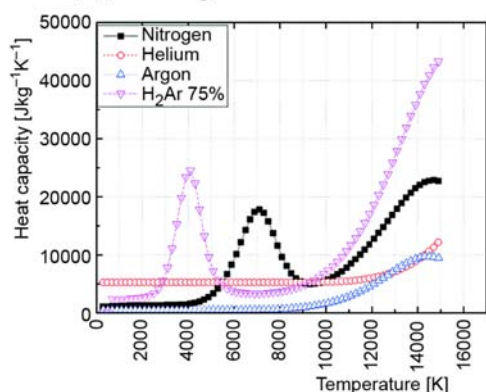


**Figure 2. Specific heat capacity of pure gases Ar, He, N<sub>2</sub> and the mixture H<sub>2</sub>Ar75% at atmospheric pressure**  
(for color image see journal web-site)

until the onset of ionization ( $\text{Ar} \Rightarrow \text{Ar}^+ + e^-$ ), The diatomic gases exhibit dissociation peaks ( $\text{H}_2 \Rightarrow 2\text{H}$ ). In the model,  $c_p$  is linearized piecewise.

The thermal conductivity behavior of gas (fig. 3) reproduces the specific heat quite accurately. It should be noted that the thermal conductivity of helium is much larger than other gas in 300 K. In the model,  $\kappa$  therefore, is linearized piecewise.

The thermal treatment of particles in a plasma medium depends not only on the operating the torch parameters but also on thermodynamic and transport properties of the plasma gas (such as heat capacity, thermal conductivity, and dynamic viscosity). The latter, is highly non-linear over all the expected temperature range and it is useful to clarify it according to the gas mixture used. The gases, most commonly used, are the monatomic gases (argon, helium) and diatomic gases (hydrogen, nitrogen) and their binary mixtures Ar-H<sub>2</sub>, Ar-He, and H<sub>2</sub>-N<sub>2</sub>. The data used in this paper are extracted from the T&TWinner database [13-15].

Figure 2 illustrates the specific heat capacities behavior of the mono atomic gases (argon, helium) These capacities are almost constant

The gas dynamic viscosity increases substantially with the temperature square until the ionization temperature, after which it collapses (fig. 4). The calculations being made under it are represented by the typical function [14, 15]  $\mu(T) = \mu(300)(T/300)^{1/2}$ .

### Results and discussions

The computed distributions with direct numerical simulation of plasma velocity and temperature for case of inlet gas velocity at x-y-plane of  $z = 0$  are shown in figs. 5. Similar profiles of plasma velocity and temperature are found in 2-D axisymmetric simulations. Numerical results for Nusselt number for particle obtained are shown in figs. 6, 7, and 8.

For the plasma gas  $H_2$  25%Ar75% (fig. 5), the Nusselt numbers are plotted for both cases (numerical simulation and correlations proposed by the authors listed in tab. 1). When analyzing the numerical results obtained it can be noticed that the Ranz and Marshall [8] correlation values are most higher than the values obtained by other correlations. The values obtained by Fiszdon [in 9 and 11] and Kalganova [in 12] models are very low, which explains why Lee and Pfender [in 11] added a corrective term to Fiszdon model (tab. 1). The results obtained by Lewis and Gauvin [12] correlation are close to our simulation values and they are in agreement with those estimated by Lee and Pfender [in 11] correlation for  $Re^{0.5}Pr^{0.33} \geq 60$ .

In the case monatomic plasma gas such as helium (fig. 7). We notice that all correlations and simulated values are lower than those obtained by the Lewis and Gauvin [12] model.

For the argon, another mono atomic plasma gas, fig. 8 shows that all correlations agree well with our results in a wide range except the cases of Lewis and Gauvin [12] and Kalganova [in 12] models. As we can notice, every correlation leads to different results according to the nature of the plasma gas used. This is why we need to obtain a unified formulation valid for all plasma gas. In this context, we proposed a new Nusselt correlation number given us:

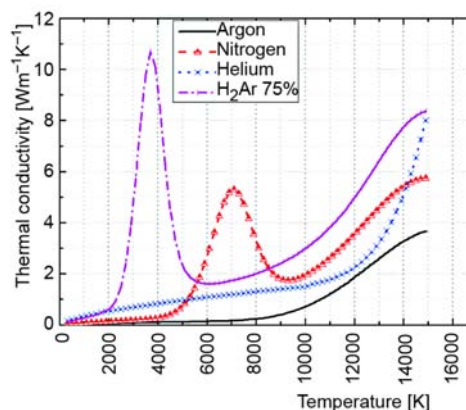


Figure 3. Thermal conductivity of pure gases Ar, He,  $N_2$  and the mixture  $H_2$ Ar75% at atmospheric pressure  
 (for color image see journal web-site)

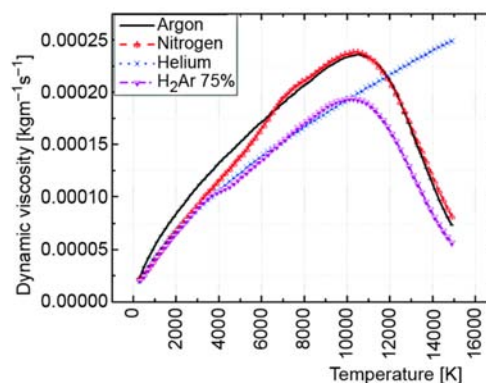


Figure 4. Atmospheric pressure dynamic viscosity of pure gases Ar, He,  $N_2$  and the mixture  $H_2$ Ar75%  
 (for color image see journal web-site)

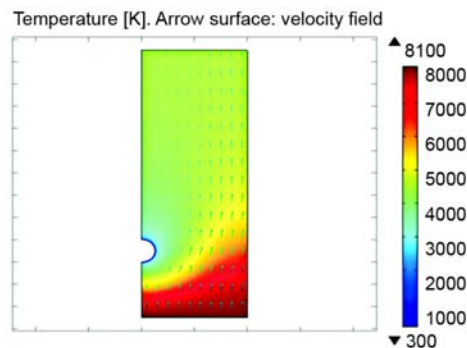


Figure 5. Illustration of the simulated temperature and velocity fields  
 (for color image see journal web-site)

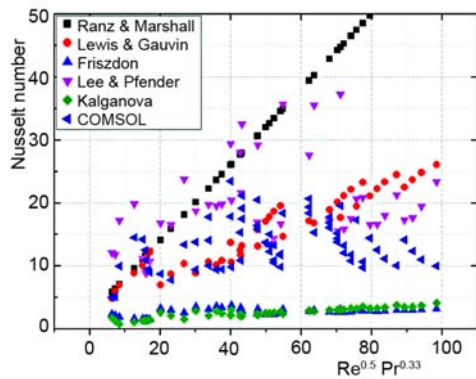


Figure 6. Nusselt number correlations as a function of Reynolds and Prandtl numbers for  $H_2Ar75\%$  (for color image see journal web-site)

$$Nu = h \frac{d_p}{K} = a + c Re^m Pr^n Y^i \quad (7)$$

The term  $Y$  introduced in eq. (7) given by the formula  $Y = \rho_\infty \mu_\infty / \rho_w \mu_w$  also appears in other correlations.

The unknown coefficients  $n$ ,  $m$ , and  $i$  can be obtained by using a multiple linear regression according to eq. (8):

$$\log(Nu - 2) = \log(c) + m \log(Re) + n \log(Pr) + i \log(Y) \quad (8)$$

Equation (7) can also be written in the following form  $Nu = A + X$ , and it is possible to evaluate the variable  $X$ , such as that:

$$X = c Re^m Pr^n Y^i \quad (9)$$

The unknown constant  $a$  in eq. (7) can also be obtained by a multiple linear regression between the values of Nusselt numbers obtained with COMSOL (which we denote  $Nu_C$ ) and  $X$  as the independent variable.

The new correlation “present model” obtained and the others cited in tab. 1 are represented as a function of  $Nu_C$ .

In figs. 9 and 10 we can see that for mono-atomic plasma gases (helium and argon), data correlations proposed by various authors including our new proposed model are concentrated around the  $Nu_C$  values except for the case of Lewis and Gauvin [12] for  $Nu_C > 4$ .

For diatomic gases, Argon-Hydrogen ( $H_2Ar75\%$ ) (fig. 11), we note that there is a wide dispersion of Nusselt values compared to the values given by the numerical simulation ( $Nu_C$ ) except the cases of Lewis and Gauvin [12], Lee and Pfender [in 11] and our proposed model, which agree well for  $Nu_C \leq 15$ .

Figure 12 summarizes results for all correlations and plasma gases used, we note that the present model results obtained agree well with the numerical simulation ( $Nu_C$ ). The correlation values from the authors cited above are relatively dispersed except for  $Nu_C \leq 10$ .

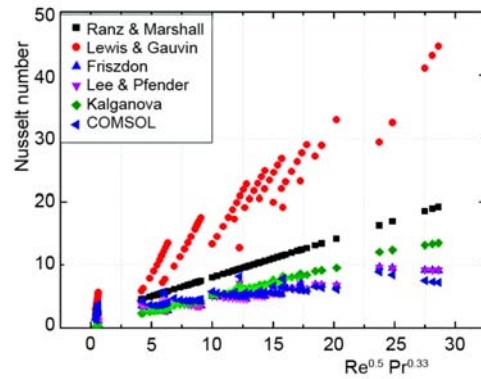


Figure 7. Nusselt number correlations as a function of Reynolds and Prandtl numbers for helium (for color image see journal web-site)

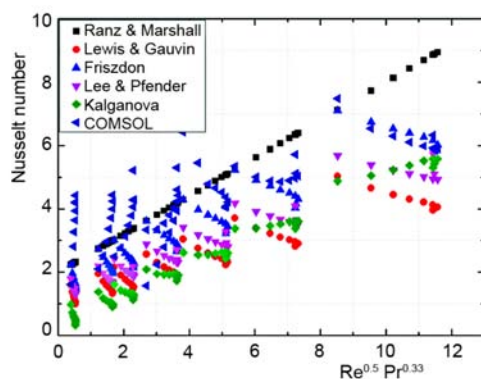
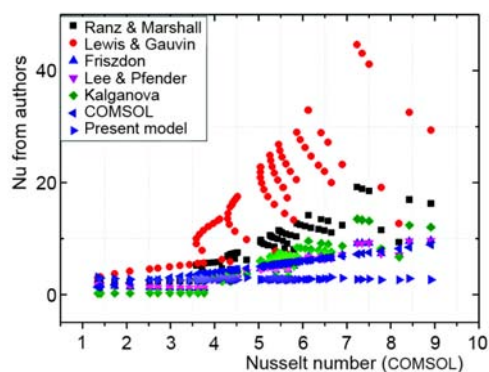
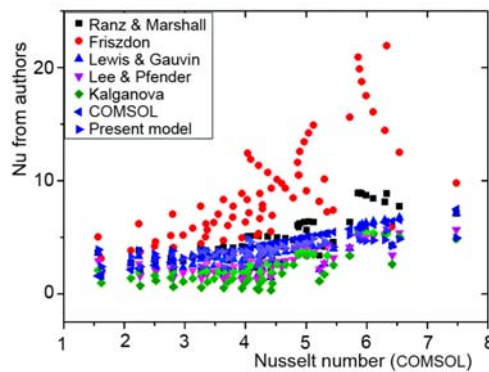


Figure 8. Nusselt number correlations as a function of  $Re$  and  $Pr$  for argon (for color image see journal web-site)



**Figure 9.** Nusselt number correlations as a function of  $Nu_C$  for helium  
 (for color image see journal web-site)



**Figure 10.** Nusselt number correlations as a function of  $Nu_C$  for argon  
 (for color image see journal web-site)

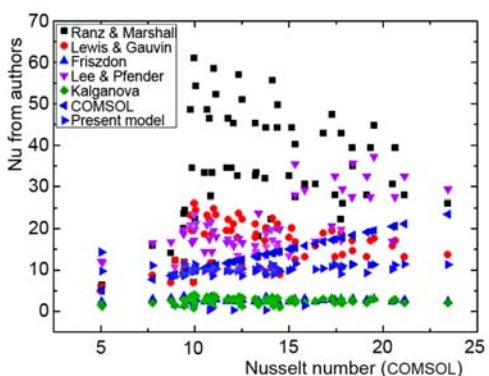


**Figure 11.** Nusselt number correlations as a function of  $Nu_C$  for  $H_2Ar75\%$   
 (for color image see journal web-site)

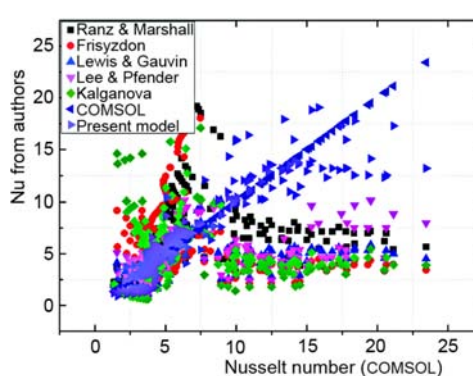


**Figure 12.** Nusselt number correlations as a function of  $Nu_C$  for all gases  
 (for color image see journal web-site)

Table 2 represents the coefficients values of eq. (7) obtained by a multiple linear regression. As we can observe in this table, each gas has its own correlation coefficients. Indeed, this is what prompted us to perform a linear regression on all the gas, and the result is indicated in the last row of the table.

**Table 2.** Values of the constants  $a$ ,  $c$ ,  $m$ ,  $n$ , and  $i$  from the proposed model presented

	$a$	$c$	$m$	$n$	$i$
Argon	4.73	0.36	0.105	-0.254	-2.05
Helium	5.25	0.563	0.138	0.762	0.104
$H_2Ar75\%$	8.85	0.142	0.4606	-0.894	-1.44
All gases	7.48	0.25	1.32	-1.1	-0.015

## Conclusions

A computational fluid dynamics code, COMSOL multiphysics software was used to explore aspects related to heat transfer from spherical particle and its surrounding atmosphere at high temperature for different gases. We studied the validity of the correlations proposed by different authors to correct the Ranz and Marshall [8] correlation. It appears that the interac-



tion of the plasma jet and spherical particles involves several complex mechanisms as the gas properties are non-linear, especially for diatomic constituents. The results show that neither the correlations derived from Ranz and Marshall [8], nor the present model is completely valid for the whole range of gas compositions and for all ranges of velocity and temperature. However, the new model presented here gives better results than previous correlations reported in the literature.

## References

- [1] Pawlowski, L., *The Science and Engineering of Thermal Spray Coatings*, John Wiley and Son, New York, USA, 1995
- [2] Zhu, Y., et al., Transient Thermal Analysis and Coating Formation Simulation of Thermal Spray Process by Finite Difference Method, *Surface and Coatings Technology Journal*, 200 (2006), 16-17, pp. 4665-4673
- [3] Mingheng, Li., Christofides, D., Computational Study of Particle in-Flight Behavior in the HVOF Thermal Spray Process, *Chemical Engineering Science*, 61 (2006), 19, pp. 6540-6552
- [4] Pfender, E., Particle Behavior in Thermal Plasma, *Plasma Chem. and Plasma Proc.* 9, (1989), S1, pp. S167-S194
- [5] Dyshlovenko, S., et al., Modeling of Plasma Particle Interactions and Coating Growth for Plasma Spraying of Hydroxyapatite, *Surface and Coatings Technology Journal*, 200 (2006), May, pp. 3757-3769
- [6] Cedelle, J., et al., Investigation of Plasma Sprayed Coatings Formation by Visualization of Droplet Impact and Splashing on a Smooth Substrate, *IEEE Transactions on Plasma Science*, 33 (2005), 2, pp. 414-415
- [7] Rojas, J. R., et al., Numerical Simulation of the Melting of Particle Injected in a Plasma Jet, *Ingeniare. Revistachilena de Ingenieria*, 17 (2009), 3, pp. 299-308
- [8] Ranz, W. E., Marshall, W. R., Evaporation from Drops, *Chem. Eng. Prog*, 48 (1952), 22, pp. 141-146
- [9] Ben Ettouil, F., et al., Predicting Dynamic and Thermal Histories of Agglomerated Particles Injected within a D. C. Plasma Jet, *Surface and Coatings Technology Journal*, 202 (2008), 18, pp. 4491-4495
- [10] Pateyron, B., et al., Influence of Water and Ethanol on Transport Properties of the Jets Used in Suspension Plasma Spraying, *Surface and Coatings Technology*, 220 (2013), Apr., pp. 257-260
- [11] Young, R. M., Pfender, E., Nusselt Number Correlations for Heat Transfer to Small Spheres in Thermal Plasma Flows, *Plasma Chemistry and Plasma Processing*, 7 (1987), 2, pp. 211-227
- [12] Lewis, A., Gauvin, W. H., Motion of Particles Entrained in a Plasma Jet, *AIChE Journal*, 19 (1973), 5, pp. 982-990
- [13] Delluc, G., et al., Modelling of Plasma Jet and Particle Behaviour in Spraying Conditions, *Proceedings*, 16<sup>th</sup> International Thermal Spray Conference, Osaka, Japan, 2004, pp. 800-805
- [14] Pateyron, B., et al., T and T Winner, the Chemistry of On-Line Transport Properties in Interval of 300 K to 20.000 K (in France), *Mécanique et Industries*, 6 (2005), pp. 651-654
- [15] Pateyron, B., Delluc, G., Logiciel TTWinner, ADEP Banque de données de l'Université de Limoges et du CNRS. (Ed.), <http://www.ttwinner.free.fr>